Arch. Mech., **53**, 4-5, pp. 421–437, Warszawa 2001

The dispacement discontinuity technique in fracture mechanics: the subsurface crack problem

S. K. KOURKOULIS[1] and G. E. EXADAKTYLOS[2]

[1] *National Technical University of Athens,*
Department of Mechanics,
Zografou Campus, Theocaris Building,
157 73 Zografou, Athens, Greece.

[2] *Technical University of Crete,*
Department of Mineral Resources Engineering
731 00 Chania, Crete, Greece.

THE DISPLACEMENT DISCONTINUITY technique is employed for the determination of the critical conditions causing propagation of a preexisting finite fracture that lies close to the free boundary of a semi-infinite medium. The technique is applied by using a suitably adapted commercial indirect boundary element code, permitting the determination of the displace-ment, strain and stress fields in multiply-connected elastic bodies. The critical conditions are then determined by employing a suitable failure criterion. The results of the numerical analysis are compared with the respective ones obtained from a series of experiments with pre-cracked specimens simulating the semi-infinite medium. The agreement is proved to be satisfactory.

1. Introduction

ALTHOUGH FRACTURE MECHANICS is accepted nowadays as one of the most reliable tools for the prediction of failure conditions of engineering structures containing defects, and many problems of practical interest related to the influence of crack-type defects on the strength and structural integrity of structures have been solved, a number of important problems related to cracked bodies of finite dimensions remain yet unanswered. The main reason is the fact that the analytical determination of the strain and stress fields in case of finite or semi-infinite cracked bodies is very difficult, preventing the application of fracture mechanics criteria for the prediction of the conditions of catastrophic crack propagation. In such cases, uncertainties in fracture mechanics analyses appear in the determination of fracture toughness, stress and strain fields, stress intensity factors etc. [1]. It seems that for these problems, the numerical methods and

techniques constitute a unique means for an, at least approximate, solution of the problem.

Such a problem that reappeared recently in the limelight and attracted the interest of engineers due to its broad field of applications in Structural- as well as in Geotechnical- and Earthquake Engineering, is that of a slightly inclined, finite subsurface crack in a semi-infinite medium. This is because strong indications exist that the relative configuration simulates in a satisfactory manner the behaviour of shallow geological faults under the influence of seismic loading, and the critical conditions leading to catastrophic crack propa-gation could provide useful information on the conditions causing activation of such faults.

It is clear that the exact full-field solution of the problem is very complicated even for a purely elastic material, due to the interaction of the crack with the free boundary of the medium. For this reason, the main qualitative features of the problem are explored here numerically, by performing plane-stress displacement discontinuity calculations. The method adopted is the Displacement Discontinuity Technique introduced originally by Crouch [2]. The technique is based on a solution that expresses the displacements and stresses at a point of the loaded cracked elastic body due to a constant displacement discontinuity over a line segment within an elastic body. The constant displacement discontinuity elements have the advantage of simplicity and are widely used for analyzing various engineering problems.

The efficiency of the technique in treating the crack problems was verified in the present work, by employing either already known closed-form solutions (cracks in infinite media [3]), or well established numerical analyses (single edge-notched specimens of finite dimensions [4]). The criterion adopted for the prediction of the critical conditions (load causing crack initiation and initial angle of crack propagation) is the T-criterion of failure [5]. The agreement between the existing results and those of the present analysis was very satisfactory, supporting the decision to use the technique for the solution of the finite subsurface crack within a semi-infinite medium.

However, and in order to verify further the results of this analysis, series of experiments were executed using specimens of suitable configuration that simulated the semi-infinite medium with a sub-surface crack. Specific configurations were selected concerning the crack inclination, in order to draw conclusions useful for the geotechnical community. As it will be seen, the experimental results for both critical quantities (load and angle) are very close to the results obtained from the numerical analysis.

2. Numerical analysis

The problem considered is demonstrated in Fig. 1: A stationary crack, AB, of length 2a is located close to the free boundary of a semi-infinite plane elastic medium. The crack is inclined with respect to the free boundary by an angle β and its mid-point is located at a distance y_0 from the boundary. The system is subjected to a uniformly applied remote tensile load P parallel to the free boundary. According to the Displacement Discontinuity Technique, the natural crack with parallel lips is considered as a linear mathematical discontinuity and the solution of the problem of a cracked semi-infinite body is obtained on the basis of the corresponding one for an infinite cracked body.

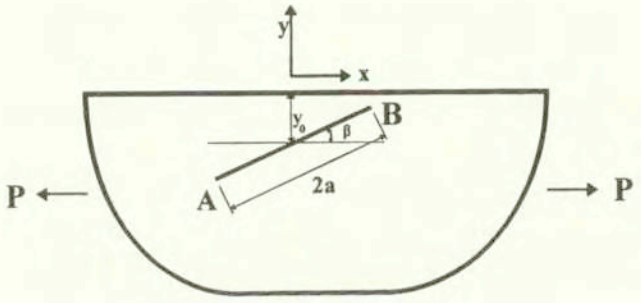

FIG. 1. Configuration of the problem.

Consider first a crack within an infinite homogeneous medium, located, for simplicity, along the y=0 line at -a⩽x⩽a (for inclined cracks, a simple coordinates transformation is performed). The crack is divided into N elementary segments and the displacements due to each segment are calculated at any point of the body, so that the general solution of the static problem is obtained a the sum of the respective elementary displacements. Practically the technique is applied in three discrete steps: (i) The coordinates of all boundary elements are defined and the respective boundary conditions are prescribed. (ii) The boundary influence coefficients are calculated and the algebraic system of equations is formulated and solved. (iii) The values of the unknown displacements and stresses are calculated in each boundary element and the analysis is extended to cover any point of the studied body.

The displacement caused by each elementary segment is written as:

$$D_i = u_i(x_i, 0_-) - u_i(x_i, 0_+), \quad \text{for } y = 0, \ i = x, y. \tag{2.1}$$

Crouch [2, 6] proved that in such a case, the displacements are given by the formula:

$$
\begin{aligned}
u_x &= D_x[2(1-\nu) f_{,y} - y f_{,xx}] + D_y[-(1-2\nu) f_{,x} - y f_{,xy}], \\
u_y &= D_x[(1-2\nu) f_{,x} - y f_{,xy}] + D_y[2(1-\nu) f_{,y} - y f_{,yy}],
\end{aligned} \tag{2.2}
$$

while the stress field is described by the following set of equations:

$$
\begin{aligned}
\sigma_{xx} &= 2GD_x(2f_{,xy} + y f_{,xyy}) + 2GD_y(f_{,yy} + y f_{,xyy}), \\
\sigma_{yy} &= 2GD_x(-y f_{,xy}) + 2GD_y(f_{,yy} - y f_{,xyy}), \\
\sigma_{xy} &= 2GD_x(2f_{,yy} + y f_{,xyy}) + 2GD_y(-y f_{,xyy}),
\end{aligned} \tag{2.3}
$$

where G and ν are the shear modulus and Poisson's ratio of the material, respectively, and the indices after the comma denote partial differentiation. Concerning the factor $f(x,y)$, it holds:

$$
\begin{aligned}
f(x,y) = \frac{-1}{4\pi(1-\nu)} \Bigg[& y\left(\arctan\frac{y}{x-a} - \arctan\frac{y}{x+a}\right) \\
& -(x-a)\ell n\sqrt{(x-a)^2+y^2} + (x+a)\ell n\sqrt{(x+a)^2+y^2}\Bigg],
\end{aligned} \tag{2.4}
$$

By superposition, the stress at the mid-point of the i-th crack element, due to displacement discontinuities at all N-elements, will be equal to:

$$
\sigma_{yy}(x^i, 0) = \sigma^i_{yy} = \sum_{j=1}^{N} \overset{ij}{A}\, \overset{j}{D}_y, \tag{2.5}
$$

where the matrix is the respective coefficient of influence and is equal to

$$
\overset{ij}{A} = \frac{-G}{\pi(1-\nu)} \frac{\overset{j}{a}}{\left(\overset{i}{x} - \overset{j}{x}\right)^2 - \overset{j}{\alpha}^2}. \tag{2.6}
$$

The coefficient $\overset{ij}{A}$ for example, gives the actual normal stress at the midpoint of the i-th segment due to a constant unit normal displacement discontinuity applied to the j-th segment ($\overset{j}{D}_y = 1$). For the case of uniformly pressurized straight crack, the stress is specified by the following system of N simultaneous linear equations in N unknowns:

$$\overset{i}{\sigma}_{yy} = -p = \sum_{j=1}^{N} \overset{ij}{A} \overset{j}{D}_y, \quad i = 1 \quad \text{to} \quad N. \tag{2.7}$$

These equations can be solved for $\overset{i}{D}_y$, i=1 to N, by standard methods of numerical analysis.

The solution for the case of an infinite cracked body being known, the problem of the semi-infinite medium with a subsurface crack can be solved by treating the surface-line of the half plane like any other boundary line and dividing it into elements following the usual process. The analytical solution to this problem can be obtained by using a procedure known as the method of images which is based on the principle of superposition. According to this method, the solution to the problem is obtained in two stages:

• An infinite plate is considered containing two symmetric cracks, as it is shown in Fig. 2. The first one is located on the negative half-plane and corresponds to the real crack, the coordinates of its mid-point being (x_0, y_0), while the second one is located on the positive half-plane and is symmetric to the first one with respect to the x-axis, i.e. the free boundary. Due to the symmetry of the configuration, the shear stresses σ_{xy} along the x-axis are zero.

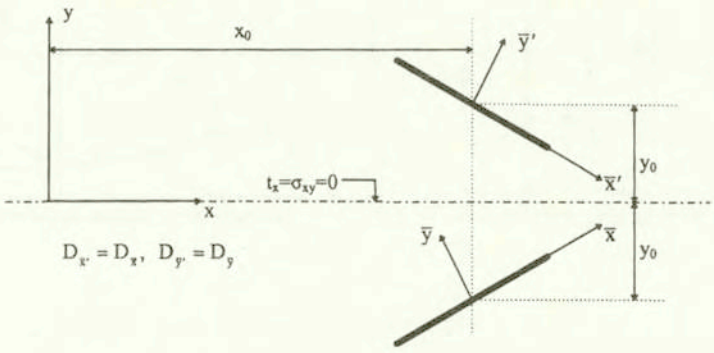

FIG. 2. Schematic representation of the method of images.

• The normal stress σ_{yy} along the x-axis is cancelled out by superimposing an additional assumption related to the elastic half-plane with prescribed tractions, t_x=0, $t_y \neq 0$. Accordingly, and denoting the displacements and stresses due to the actual displacement discontinuity u_i^A and σ_{ij}^A those due to its image u_i^I and σ_{ij}^I, and the ones resulting from the supplementary retraction solution $u\,i^S$ and

σ_{ij}^S, the complete solution for the half-plane $y \leqslant 0$ becomes:

$$u_i = u_i^A + u_i^I + u_i^S,$$
$$\sigma_{ij} = \sigma_{ij}^A + \sigma_{ij}^I + \sigma_{ij}^S. \tag{2.8}$$

The results of the numerical analysis concerning the strain distribution have been plotted in Fig. 3(a,b) for an external load level P equal to 80% of the final fracture load. The configuration studied corresponds to a crack of length equal to 2a=20 mm, inclined by an angle β=10^o with respect to the free boundary, the mid-point of which is located at a distance $|y_0|$=20 mm from the free surface (Fig. 1). The specific configuration is chosen since most geological faults, either normal or the thrust ones, are relatively slightly inclined with respect to the Earth's surface. Since from the point of view of geotechnical engineering, the interest is focussed mainly on the variation of strains along the directions parallel

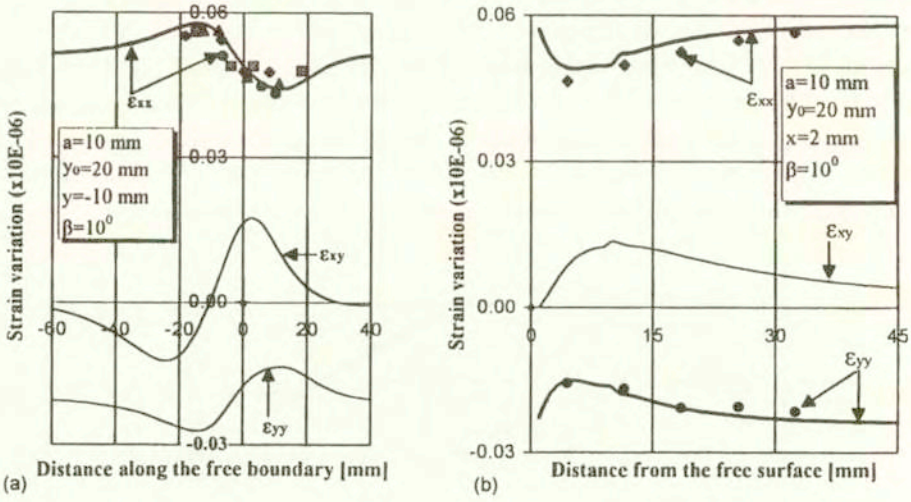

FIG. 3. Strain distribution along a line.

and perpendicular to the free surface, the familiar in Fracture Mechanics polar plot of the strain distribution around the crack tip is avoided in the present work. Thus, all three strain components are plotted in Fig. 3a along a line parallel to the free surface of the medium at a distance y=-10 mm from it, while in Fig. 3b the respective quantities are plotted along a line perpendicular to the free surface at a distance x=2mm from the tip nearest to the boundary (tip B in Fig. 2). In the same figures, the corresponding experimental results have been plotted. Although analytical discussion of the experimental results follows in

the next section, it can be said that the agreement between the numerical and experimental results is satisfactory.

It can be seen from Fig. 3a that the disturbance of the strain field due to the free boundary is of dominant importance, since the symmetry of distribution for all three strain components disappears. On the other hand, it is observed that the strain components show clearly the extreme values (maximum or minimum) as the crack tips are approached, but it is to be emphasized that the points where the maximum values are reached are not located exactly above the crack tips. A similar conclusion is drawn from Fig. 3b, especially for the shear strain ε_{xy}, the maximum value of which does not correspond to the point straight forward along the axis of the crack.

In the next Fig. 4, the polar distribution of the stress components according to the numerical analysis is plotted for the same configuration ($2a$=20 mm and β=10^0) and for both crack tips: thick lines correspond to the tip A while the thinner ones to the tip B

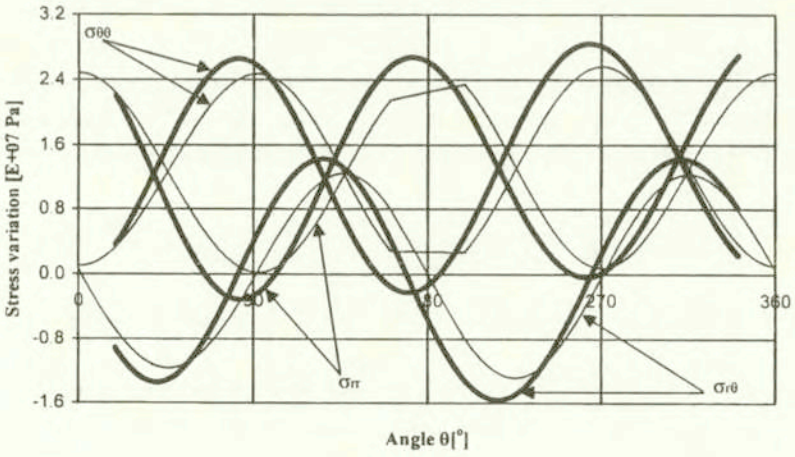

FIG. 4. Polar distribution of the stress components around tip A (thick lines) and tip B (thin lines).

It is again obvious that the two sets of lines are not identical as it should be expected in case of an infinite medium, exactly due to the presence of the free boundary. From this figure one could obtain directly the expected crack initiation angle according to the maximum tangential stress criterion (σ_θ-criterion) as $\theta_{A,\sigma}$=86^o and $\theta_{B,\sigma}$=93^o, which, as it will be seen in next section, are slightly higher than the respective experimental values $\theta_{A,\text{exp}}$=81^o and $\theta_{B,\text{exp}}$=87^o.

3. The failure criterion and the critical conditions

The stress and strain fields having been calculated, a failure criterion is required to predict the onset of crack propagation and the initial propagation angle. A number of criteria have been proposed towards this direction during the past decades. For the purposes of the present study the T-criterion of failure was used [5], mainly due to its clear physical meaning and the fact that its predictions for the critical load and for the initiation angle have been found to be in a very good agreement with the experimental evidence, both for centrally cracked and single-edge notched specimens [7]. For comparison reasons, the σ_θ-criterion (maximum tangential stress criterion [8]) was also used together with the T-criterion, in some cases.

The T-criterion of failure is based on the following assumptions: (i) The crack propagates towards the direction θ_o of the maximum value of the density of the elastic dilatational strain energy T_V. The propagation starts when this maximum value exceeds a critical limit $T_{V,0}$. (ii) The polar distribution of T_V around the crack-tip is calculated along the elastic-plastic boundary, where the distortional strain energy density, T_D, is constant, equal to a critical value $T_{D,0}$ and finally (iii) Both $T_{V,0}$ and $T_{D,0}$ are considered as material constants determined experimentally, according to the procedure described in [9].

Mathematically speaking, and for plane stress conditions, like the ones prevailing in the present study, the criterion is expressed as follows:

$$T_V\left(r\left(\vartheta\right),\vartheta\right)\big|_{\vartheta=\vartheta_o} \geqslant T_{V,0} = \text{const.} \tag{3.1}$$

$$\left.\frac{\partial T_V\left(r\left(\vartheta\right),\vartheta\right)}{\partial\vartheta}\right|_{\vartheta=\vartheta_o} = 0, \quad \left.\frac{\partial^2 T_V\left(r\left(\vartheta\right),\vartheta\right)}{\partial\vartheta^2}\right|_{\vartheta=\vartheta_o} \leqslant 0, \tag{3.2}$$

$$T_D = \frac{1+\nu}{3E}\sigma_\Delta^2 = T_{D,0} = \text{const.} \tag{3.3}$$

The polar variation of the quantity controlling the crack initiation according to the T-criterion, namely the elastic dilatational strain energy density, T_v is plotted in Fig. 5, for both tips A and B of the crack, for β=10^0, y_0=20 mm and $2a$=20 mm. The main characteristic is that the distortion of the shape of the distribution, inevitably caused by the inclination of the crack, is balanced by the influence of the free boundary. Since this influence is more pronounced at the tip B, the distribution of the elastic dilatational strain energy density at this tip is almost circular. Such a balance is not possible for tip A, since its distance from

the free surface is greater. From the same figure it is also concluded that the expected angles of crack initiation according to the T-criterion, are $\theta_{A,T}=83^o$ and $\theta_{B,T}=89^o$, for tips A and B respectively, which are close enough to the experimental results.

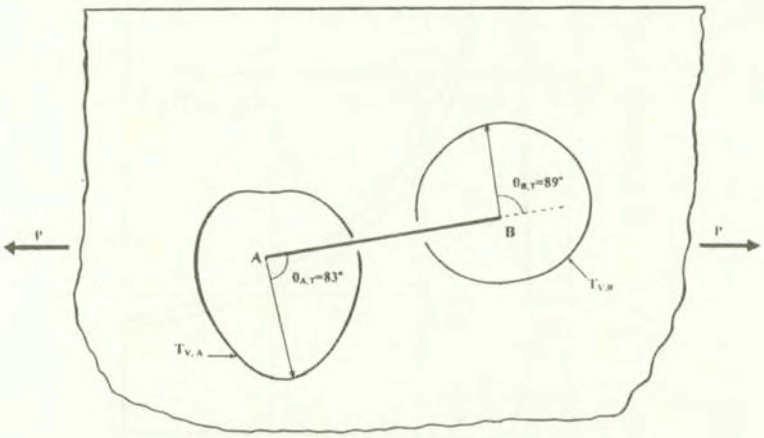

FIG. 5. Polar distribution of the elastic dilatational strain energy density around the two crack tips.

Concerning the critical load, what is most important is the detection of the configuration for which the crack is either most eager or most reluctant to propagate. For this purpose, the variation of the square root of the elastic dilatational strain energy density, reduced over the respective quantity for an infinite medium, is plotted in Fig. 6, versus the reduced distance of the mid-point of the crack, y_0, from the free boundary, since this quantity is directly related to the critical fracture load. The configuration corresponds again to $\beta=10^0$, $2a = 20$ mm while the position of the mid-point of the crack varies from $y_c = a\sin\beta$, corresponding to a single-edge notched configuration, to $y_c = 12a$, corresponding to a configuration which starts resembling the infinite medium. It is concluded from this figure that the critical condition is first fulfilled at the tip A, i.e. the one most remote from the free boundary. This tendency is decreased as the crack moves towards the interior of the medium, since the influence of the boundary becomes weaker and the displacement distribution around the two tips becomes symmetric.

However, what is most interesting, and perhaps astonishing, from the analysis of the variation of the square root of the elastic dilatational strain energy density versus the position of the crack, is that this function is not a monotonic one. Specific configurations exist for which the crack appears to be most reluctant

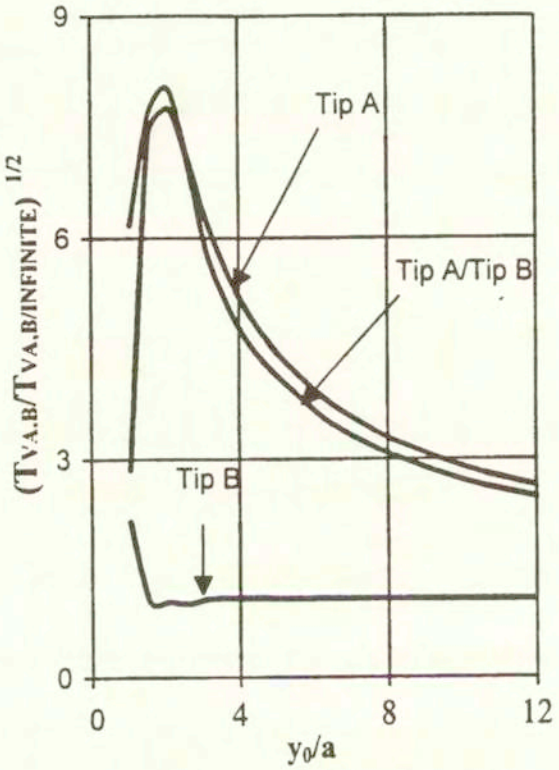

FIG. 6. Variation of the reduced elastic dilatational strain energy density around the two crack tips versus the position of the crack.

to propagate. For example, for the case studied in Fig. 6, the relative function shows a clear maximum for cracks located at a distance $y_c \cong 2a$ from the free boundary. It means that such a geometry is much more stable compared to both the centrally cracked finite or infinite medium and the single-edge notched geometry. Such a conclusion, perhaps contradicting the common sense, was the main motive for an extended experimental analysis of the phenomenon, the results of which are presented in the next section.

4. Experimental procedure and results

Series of uniaxial tension tests were carried out using the specimens, shown schematically in Fig. 7, i.e. internally cracked plates of dimensions 0.300 x 0.275 x 0.002 m^3. Two crack inclinations were selected: One with $\beta=10^0$, i.e. cracks

that are sub-parallel to the free boundary, fulfilling the demands of geotechnical engineers, for the case of geological faults that are slightly dipping with respect to the surface of the earth, and one with $\beta=90^0$, i.e. faults that dip 90^0, for comparison reasons. The length of the cracks was $2a = 20$ mm and their location varied from single-edge notched specimens to centrally cracked ones.

As it is seen from Fig. 7, the dimensions of the specimens were selected in such a way, that the geometry simulated satisfactorily the semi-infinite body with a subsurface crack. Special attention was paid to ensure that the stress waves reflected from the three boundaries, other than the one closest to the crack, arrived to the crack-tips after the crack emanating from tip B had reached the free boundary (ff). On the other hand, the very small thickness of the plate ensured that the loading conditions could be safely considered as plane-stress ones.

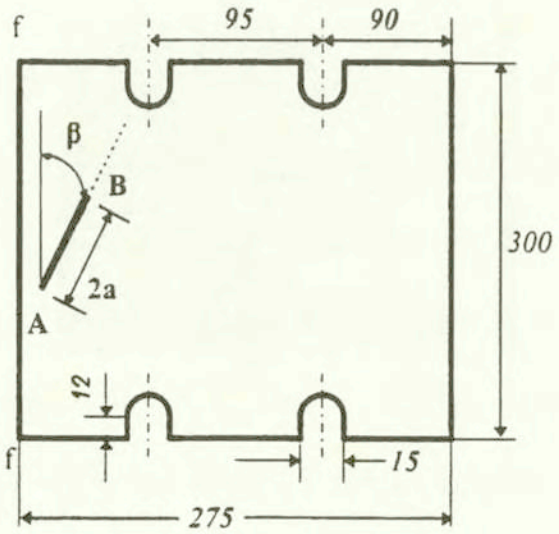

FIG. 7. Geometry of the specimens

The material used in the experimental study was Polymethylmethylate (PMMA), known under the commercial name Plexiglas. The reason for this choice is that the specific material is extremely brittle and behaves in a linear elastic manner from the very early loading steps up to almost the final failure. Since the mechanical properties of this material vary significantly, depending on its exact chemical composition, the properties of the batch used were determined with the aid of a preliminary series of standardized uniaxial tension tests. From

these experiments it was concluded that the assumptions of Linear Elastic Fracture Mechanics, adopted in the previous sections, were absolutely justified. The results of these tests are summarized in Table 1.

Table 1. The mechanical properties of Plexiglas (PMMA).

Elasticity modulus, E	3.8 GPa
Shear Modulus, G	1.5 GPa
Poisson's ratio, ν	0.35
Fracture Stress, σ_f	88.0 MPa
Velocity of longitudinal waves, c_l	2730 m/s
Velocity of transverse waves, c_t	1430 m/s

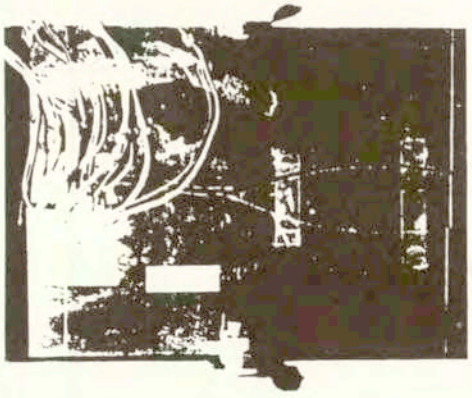

FIG. 8. A fractured specimen with the arrangement of strain gauges.

The experiments were carried out with the aid of an Instron loading frame with maximum loading capacity $25\text{x}10^4$ N. Taking into account that the maximum fracture load recorded during the whole series of tests did not exceed in any case the level of $2\text{x}10^4$ N, it is concluded that the stiffness of the frame could be considered infinite. The load was applied statically and it was parallel to the free boundary (ff) of the specimen. For each geometry (crack inclination, β, and initial crack length, $2a$), seven different classes of tests were carried out, with the free parameter, the distance of the center of the crack from the free boundary of the specimen, y_0. Five to ten specimens were tested for each class, depending on the repeatability of the results. The characteristics recorded during each test were the critical load causing crack initiation, P_{cr}, and the angle

(a)

(b)

FIG. 9. Fractured specimens with $\beta = 10^0$ and (a) $y_0 = 2a$ (b) $y_0 = 6a$.

of the initial crack propagation from the two tips A and B, θ_A and θ_B, respectively. In a number of tests, the variation of the strain field in the vicinity of the crack tips was also recorded during the loading procedure, using a system of six to ten orthogonal strain rosettes, suitably attached at various strategic points of the specimens. The gauges were arranged along a line either parallel or normal to the free boundary of the specimens. In Fig. 8, a characteristic photograph of a fractured specimen is shown indicating both the arrangement of the strain gauges and the branching phenomenon that accompanied systematically the fracture process. In Fig. 9 (a,b), two characteristic fractured specimens are shown corresponding to $\beta=10^0$ and $y_0 = 2a$ mm (Fig. 9a) and $y_0 = 6a$ (Fig. 9b).

The experimental results obtained from the strain gauge rosettes have already been plotted in Fig. 3(a, b). The agreement between the numerically obtained values for the strain components and the respective experimental quantities is very satisfactory, indicating the validity of the technique used for the numerical solution.

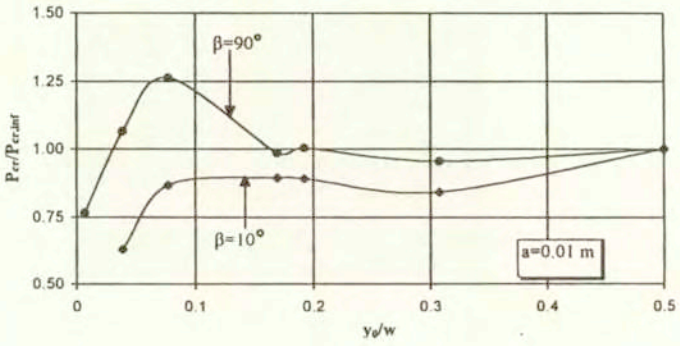

FIG. 10. Reduced critical load versus the position of the crack.

In Fig. 10 the experimentally obtained critical load, P_{cr}, is plotted versus the distance of the center of the crack from the free boundary, y_0, for both the tested configurations, i.e. β=90^o and β=10^o. The values of the critical load are reduced over the respective value for the case of a centrally cracked specimen of the same geometry, while the geometric parameter, y_0, is reduced over the width of the plate, w. It can be seen from this figure that for both configurations, the critical load is not a monotonous function of the distance of the crack from the free boundary, exactly as it was indicated by the numerical analysis of the previous section. A characteristic weak minimum is observed at $x_c \cong 0.3w$. However, the most astonishing observation is the existence of a global maximum in the case of β=10^o, located at about $y_0^* \cong 0.075w$, which means that the specific configuration corresponds to specimens with higher resistance to fracture compared to the centrally cracked ones. Taking into account the dimensions of the crack and the width of the specimens it is concluded that the location of the global maximum is identical to that detected by the numerical analysis and the T-criterion, namely equal to $y_0^* = 2a$ (the initial crack length). It should be mentioned, however, that the scattering of the experimental results for the specific specimen's class varied around 18% while the scattering for all other classes did not exceed 5%. Motivated by this difference, additional tests were carried out for the specific configuration. Both phenomena, i.e. the high scattering and the existence of the total maximum, were consistently repeated indicating that a more thorough study is necessary in order to understand the natural basis of such a type of inherent instability.

In Fig. 11 the experimentally obtained crack initiation angles are plotted, again versus the reduced distance of the center of the crack from the free boundary, y_0, for both crack tips and for crack inclination angle β=10^o. The influence of the free boundary is again of dominant importance. For the tip closer to the free surface (tip B), the initiation angle is considerably higher as compared to

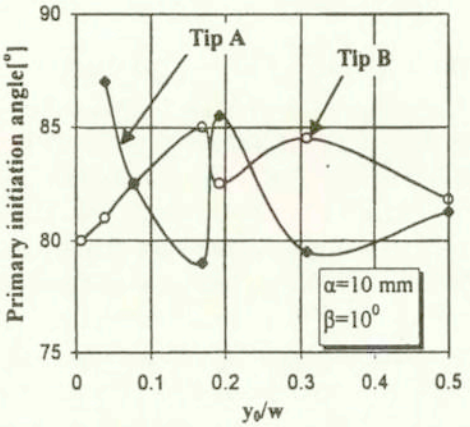

FIG. 11. Initiations angles for tips A and B.

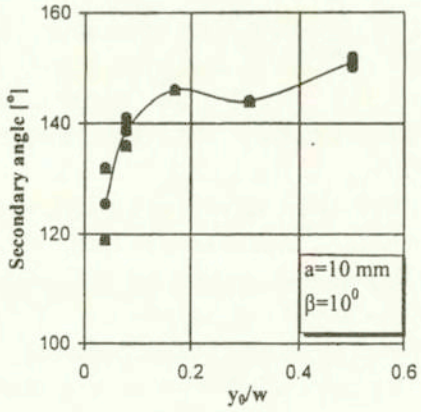

FIG. 12. Initiation angle of the secondary cracks occasionally emanating from tip A.

the respective one of the remote tip (tip A) for low y_0 values. The strong fluctuation of the values of the initiation angles should also be emphasized as well as the fact that for $y_0 = 0.5w$ the experimental values for the two tips become equal as it should be expected for symmetry reasons.

Finally, in Fig. 12 the values of the secondary (after failure) initiation angles, occasionally emanating from tip A, are plotted for the same crack inclination. The influence of the free boundary for this quantity is again dramatic.

5. Discussion and conclusions

The problem of the conditions causing catastrophic propagation of a pre-existing sub-surface crack in a semi-infinite medium was studied in the present paper, both numerically and experimentally. The main qualitative features of the problem were explored by using the displacement discontinuity technique in conjunction with a suitably adapted indirect boundary element code for the determination of the displacement, strain and stress fields around cracks in a semi-infinite, isotropic, linearly elastic half-space. The T-criterion of failure was adopted for the determination of the critical conditions at the moment of crack initiation. The results obtained from the numerical analysis were compared to the respective ones obtained experimentally. Special attention was given to a specific configuration of the specimens, i.e. those with cracks very slightly inclined with respect to the free boundary, since this configuration is supposed to simulate the geometry of a number of shallow, gently dipping geological faults, responsible for a number of catastrophic earthquakes in the Mediterranean basin. The agreement between the numerical results and the experimental evidence for the strain distribution was satisfactory. The same was true for the predictions of the T-criterion of failure, for both the critical load and the crack initiation angle.

The main advantage of the Displacement Discontinuity Technique is that it is very flexible and if it is supplemented with a suitable fracture criterion, it can be used both for the prediction of the initiation angle of a stationary crack in an elastic medium of finite dimensions as well as for the estimation of the strength of the body, i.e. the critical load that causes initiation of the crack.

However, the most attractive conclusion of the present study was that the load required to cause initiation of the crack is not a monotonic function of the distance of the center of the crack from the free boundary. Specific configurations were detected for which the crack initiation load was maximized, the conclusion contradicting perhaps the common sense. Depending on the crack inclination angle, this optimum distance varied between 2 and 2.5 times the initial semi-length of the crack. Such a conclusion, associated with a significant increase of the scattering of the experimental results, in other words with an inherent instability of the phenomenon, is not easily explainable. Further experimental study is required, for a wider class of materials, before definite conclusions are drawn.

Acknowledgements

The authors gratefully acknowledge the assistance of Mr P.-J. R. Goycoechea in the execution of the experiments.

References

1. A. R. ROSENFIELD AND C. W. MARSCHALL, *Engineering fracture mechanics,* **45**(3), 333-338, 1993.
2. S. L. CROUCH, *Solution of plane elasticity problems by the displacement discontinuity method,* International Journal of Numerical Methods in Engineering, **10,** 301-343, 1976.
3. G. R. IRWIN, *Analysis of stresses and strain near the end of a crack traversing a plate,* Journal of Applied Mechanics, **24**, 361-364, 1957.
4. Y. MURAKAMI, (editor), *Stress Intensity Factors Handbook,* Pergamon Press, Vol.**II**, p. 916, 1981.
5. N. P. ANDRIANOPOULOS and P. S. THEOCARIS, *The Griffith-Orowan fracture theory revisited: The T-criterion,* International Journal of Mechanical Science, **27**, 793-801 1985.
6. S. L. CROUCH and A. M. STARFIELD, *Boundary Element Methods in Solid Mechanics,* Allen & Unwin, London 1983.
7. P. S. THEOCARIS, N. P. ANDRIANOPOULOS and S. K. KOURKOULIS, *The angle of initiation and propagation of cracks in ductile media,* Experimental Mechanics, **27**, 120-125, 1987.
8. E. H. YOFFE, *The moving Griffith crack,* Philosophical Magazine, **42**, pp. 739-750, 1951.
9. N. P. ANDRIANOPOULOS and S. K. KOURKOULIS, *FLDs for modern Al and Al-Li alloys and MMCs,* 10^{th} Int. Conf. on Exp. Mech., J.F.GOMEZ [Ed.], Balkema, 995-1000, Rotterdam 1994.

Received November 2, 2000.